SAND2019-13897J

Spin transport in an insulating ferrimagnetic-antiferromagnetic-ferrimagnetic trilayer as a function of temperature

Yizhang Chen,[1] Egecan Cogulu,[1] Debangsu Roy,[1] Jinjun Ding,[2] Jamileh Beik Mohammadi,[1] Paul G. Kotula,[3] Nancy A. Missert,[3] Mingzhong Wu,[2] and Andrew D. Kent[1,a)]

1 Center for Quantum Phenomena, Department of Physics, New York University, New York, New York 10003, USA

2Department of Physics, Colorado State University, Fort Collins, Colorado 80523, USA
3Sandia National Laboratories, Albuquerque, New Mexico 87185, USA

ABSTRACT

We present a study of the transport properties of thermally generated spin currents in an insulating ferrimagnetic-antiferromagnetic- ferrimagnetic trilayer over a wide range of temperature. Spin currents generated by the spin Seebeck effect (SSE) in a yttrium iron garnet (YIG) YIG/NiO/YIG trilayer on a gadolinium gallium garnet (GGG) substrate were detected using the inverse spin Hall effect (ISHE) in Pt. By studying samples with different NiO thicknesses, the spin diffusion length of NiO was determined to be ~3.8 nm at room temperature. Surprisingly, a large increase of the SSE signal was observed below 30 K, and the field dependence of the signal closely follows a Brillouin function for an S=7/2 spin. The increase of the SSE signal at low temperatures could thus be associated with the paramagnetic SSE from the GGG substrate. Besides, a broad peak in the SSE response was observed around 100 K. These observations are important in understanding the generation and transport properties of spin currents through magnetic insulators and the role of a paramagnetic substrate in spin current generation.

I. INTRODUCTION

A spin current, or a flow of spin angular momentum, can be carried by conduction electrons[1,2] or spin waves.[3,4] In a material with strong spin-orbit coupling, like Pt, a spin current can be converted into a measurable voltage by the inverse spin Hall effect (ISHE).[5] Spin currents can be generated by the spin Hall effect (SHE),[6–9] spin pumping,[10] or the spin Seebeck effect.[11–14] The spin Seebeck effect refers to the generation of spin currents when a temperature gradient is applied to a magnetic material and has potential applications in converting waste heat into electricity.

A conventional spin valve consists of two ferromagnetic met- als separated by a non-magnetic metal.[15,16] Recently, a new spin valve structure based on an antiferromagnetic insulator (AFI) sand- wiched between two ferromagnetic insulators (FI) was proposed and a magnonic spin-transfer torque was predicted.[17,18] Experi- ments showed the magnonic valve effect by controlling the relative orientations of $Y_3Fe_5O_{12}$ (YIG) magnetization in a YIG/NiO/YIG

structure.[19] YIG is a ferrimagnetic insulator with low magnetic dissipation, highly efficient spin current generation,[20] and long- distance magnon transport.[21] Nickel Oxide (NiO) is an antiferro- magnetic insulator that has a face-centered curbic structure and a bulk Néel temperature of 525 K.[22,23] Below the Néel temperature, the Ni^{2+} spins are coupled ferromagnetically in {111} planes and aligned in opposite directions with adjacent planes. NiO has a biax- ial anisotropy and the magnon energies are non-degenerate at zero field.[24] However, thermally activated magnons with higher modes can transmit through NiO.[25,26] Previous experiments have shown that spin currents can be transmitted and amplified through NiO near the blocking temperature due to strong spin fluctuation in NiO and a large spin-mixing conductance at NiO/normal metal (NM) interfaces.[23,27,28]

To understand the generation, transmission, and detection of spin currents through a multilayer consisting of different mag- netic insulators, transport measurements were performed in samples with a heterostructure of GGG(500 μm)/YIG(20 nm)/NiO(t nm)/ YIG(15 nm)/Pt(5 nm), where t = 2.5, 5, 7.5, 10 nm. Here GGG ($Gd_3Ga_5O_{12}$) is the standard substrate used to grow epitaxial YIG. Above the spin-glass transition temperature (≈0.2 K), GGG is para- magnetic with no long-range magnetic order.[29,30] In addition, GGG has been shown to have a paramagnetic SSE, with a magnitude comparable to the SSE that of YIG at low temperatures.[31]

In this work, room-temperature measurements were first per- formed to characterize the spin diffusion length of NiO. The SSE sig- nal was measured from 5 to 300 K in an applied magnetic field of 1 T. The SSE response shown a broad peak around 100 K and the under- lying mechanisms are discussed. Surprisingly, a large increase of the SSE signal was observed below 30 K. Field-dependent experiments show that the SSE voltage follows a Brillouin function with a spin S=7/2 at low temperatures. This indicates that the sharp increase at low temperatures originates from the paramagnetic SSE of the GGG substrate when a strong magnetic field is applied.

II. SAMPLE FABRICATION AND MEASUREMENT TECHNIQUES

The sample was fabricated in the following way. First, a 20 nm YIG layer was grown epitaxially on a (111)-oriented GGG sub- strate (500 μm) at room temperature and annealed in O_2 at high-temperature.[32] An Ar plasma was used to clean the surface of the samples before depositing NiO via radio frequency (RF) sputtering in another chamber. Afterward, a 15 nm YIG layer was grown on top with the same growth conditions of the first layer. Then the sam- ple was capped with a 5 nm Pt layer. For transport measurements, the Pt was patterned into Hall bar structures using electron beam lithography and Ar plasma etching. The Hall bar has a width of 4 μm and the length between the two longitudinal contacts is 130 μm. An alternating current (AC) with a frequency of 953 Hz was used. The current density in this work is fixed at $j_{ac} = 1.5 \times 10^{10} A/m^2$ for all the measurements. As the temperature gradient induced by the AC oscillates at twice the frequency, the second harmonic Hall voltage $V^{2\omega}_{xy}$ measured by a lock-in amplifier is proportional to the amplitude of the SSE-produced spin current.[33,34] Room-temperature measurements were performed with a 0.4 T magnetic field applied in-plane. Temperature-

dependent measurements were carried out in the Quantum Design PPMS system also with an in-plane field.

III. EXPERIMENTAL RESULTS

Figure 1(a) is a schematic of the heterostructure GGG/YIG/ NiO/YIG/Pt. A magnetic field is applied in-plane at an angle φ with respect to the current. The cross section of the sample is charac- terized by scanning transmission electron microscopy with energy- dispersive X-ray spectroscopy, shown in Fig. 1(b). The crystal struc- ture of the sample is shown in Fig. S1 (see supplementary material). Both the top and bottom YIG layers are crystalline, with thicknesses of 15 nm and 20 nm. NiO is polycrystalline, with a thickness of 5 nm for the sample in Fig. S1.

First, $V^{2\omega}{}_{xy}$ was measured as a function of φ for samples with NiO thicknesses of 2.5, 5, 7.5, and 10 nm. $V^{2\omega}{}_{xy}$ reaches a maximum at φ = 180 and minimum at φ = 0 . This is consistent with the ISHE symmetry of the Hall voltage $V_{\mathrm{ISHE}} \propto \vec{j}_S \times \hat{\sigma} \propto \nabla T \times \hat{m} \propto \cos(\varphi)$, where $\vec{j}_S$ is the spin current, $\hat{\sigma}$ is the spin polarization direction, ∇T is the temperature gradient, and $\hat{m}$ is a unit vector in the direction of magnetization. The angular dependence of the $V^{2\omega}{}_{xy}$ was fitted with a cosine function and the amplitude $\Delta V^{2\omega}{}_{xy}$ is plotted as a function of the NiO thickness (Fig. 2). $\Delta V^{2\omega}{}_{xy}$ decays rapidly as the NiO thickness increases and is fitted to

$$V = V_{\mathrm{bottom}} e^{-t/\lambda_{\mathrm{NiO}}} + V_{\mathrm{top}}, \quad (1)$$

where V_{bottom} and V_{top} represent the SSE signal from the bottom and top YIG layers, t is the NiO thickness, and λ_{NiO} is the spin-diffusion length of NiO. Here we assume V_{top} is constant and V_{bottom} decays exponentially as a function of the NiO thickness. When NiO thick- ness is 10 nm, the SSE signal is 14.6 ± 4.9 nV, smaller but the same order as the 22.7 nV measured in a YIG(20 nm)/Pt(5 nm) bilayer with the same configuration.[33] If V_{top} is taken to be 10 nV, the char- acteristic spin diffusion length of NiO is $\lambda_{\mathrm{NiO}} \approx 3.8 \pm 0.9$ nm, close to what have been found in previous work on YIG/NiO/Pt struc- tures.[35] However, $V_{\mathrm{bottom}} = 172 \pm 39$ nV is 17 times larger than V_{top}, while the bottom YIG layer is only 1.3 times thicker than the top YIG layer. This observation indicates that the spin current gener- ated from the bottom YIG layer is enhanced as it transmits through the NiO thin layer and YIG/NiO, and NiO/YIG interfaces. Further experiments are needed to understand the mechanisms of this spin current enhancement. To further investigate the generation and transport of thermally generated spin currents through the heterostructure, the angular dependence of $V^{2\omega}{}_{xy}$ was measured from 5 to 300 K with an applied magnetic field of 1.0 T (Fig. 3(a)). The amplitude $\Delta V^{2\omega}{}_{xy}$ is extracted by the same method discussed above and plotted as a function of the temperature (Fig. 3(b)). For the 5 nm thick NiO sample, as temperature decreases from 300 to 100 K, $\Delta V^{2\omega}{}_{xy}$ increases steadily from 150 to 271 nV. From 100 to 50 K, $\Delta V^{2\omega}{}_{xy}$ slightly decreases to 257 nV, forming a broad peak around 100 K, shown in the inset of Fig. 3(b). However, as temperature decreases below 30 K, $\Delta V^{2\omega}{}_{xy}$ increases dramatically from 297 to 994 nV. The sharp increase of $\Delta V^{2\omega}{}_{xy}$ below 30 K

was observed for all samples. Similar peaks around 100 K have been observed in YIG/NM, YIG/Cu/NM, and YIG/NiO/NM.[23,25,28,37] This peak could have multiple origins. First, as temperature decreases, the magnon population decreases while the effective magnon propagation length in YIG increases. These two competing effects can give rise to a maximum in the spin cur- rents at a specific temperature.[25,36,37] Second, the large spin-mixing conductance at NiO/YIG and YIG/NM interfaces can lead to an enhancement of spin currents transmitted.[23,37] Third, the strong spin fluctuation in NiO near the blocking temperature can lead to the amplification of spin currents through NiO.[23,28]

The sharp increase of SSE signal below 30 K were absent in pre- vious experiments performed on YIG/NiO/Pt and GGG/YIG/NiO/ YIG/Pt samples.[19,23] At low temperature, the population of ther- mally activated magnons in a ferromagnet decreases as temperature decreases and goes to zero at absolute zero.[25,36] This is inconsistent with what we observed if only magnons generated in the YIG lay- ers were taken into account. However, with a magnetic field of 1 T, much higher than the fields applied in previous work,[19,23] the GGG substrate can produce a large flow of spin current due to the para- magnetic SSE.[31] At low temperatures, the SSE voltage produced in a GGG/NM bilayer is proportional to T^{-4} and follows a Brillouin function with an S=7/2 spin (Gd^{3+}).[31] Therefore, field-dependent measurements of $V^{2\omega}$ xy were carried out in the sample with 2.5 nm thick NiO to reveal how the SSE signal is related to the magnetization of the heterostructure. Fig. 4(a) shows $V^{2\omega}$ xy as a function of the applied magnetic field between -5.0 and 5.0T with temperature ranging from 5 to 50 K. At 50 K, as the applied field goes from -5.0 to -1.0 T, $V^{2\omega}$ $xy \approx 530$ nV, almost independent of the applied field. As the applied field increases from -1.0 T to 20 mT, $V^{2\omega}$ xy decreases slowly to 108 nV. Then $V^{2\omega}$ xy drops sharply to -156 nV as $\mu_0 H$ increases from 20 to 100 mT. As the applied field increases to 1.0 T, V_{xy} decreases slowly to -540 nV and again is nearly constant thereafter. Sharp switching steps can be observed in the $V^{2\omega}$ $xy - H$ curves around ± 50 mT, mainly due to the switching of the YIG magnetization. In Fig. S2 of the supplementary material, VSM measurements show that all samples have coercivity smaller than 5 mT when the magnetic field is swept at 0.2-0.3 mT/second (compared to ~10 mT/second in the transport measurements). Only one magnetization reversal can be identified between -200 and 200 mT in the $V^{2\omega}$ $xy - H$ curves, indicating the top and bottom YIG layers switch almost at the same field. As temperature decreases from 50 to 5 K, Δ $V^{2\omega}$ xy increases from 535 to 1970 nV, while the position low-field step does not change significantly. Fig. 4 shows that $V^{2\omega}$ xy qualitatively follows the Brillouin function of an S=7/2 spin (Gd^{3+}) at low temperatures. However, at higher temperatures, $V^{2\omega}$ xy deviates from the Brillouin function (see Fig. S4 in the supplementary material). The temperature and field dependence of $V^{2\omega}$ xy strongly indicates that the large increase of spin currents below 30 K originates from the paramagnetic SSE in the GGG substrate at low temperatures.

IV. DISCUSSION

The SSE voltages decay rapidly as NiO thickness increases at room temperature, as presented in Fig. 2. A model based on the spin currents generated from both the top and bottom YIG layers was proposed (Eqn. 1). The NiO spin diffusion length is determined to be ~3.8 nm, close to what has been found in YIG/NiO/Pt structures.[35] The temperature dependence of the SSE response was measured from 5 to 300 K with an applied magnetic field of 1 T. A broad peak was observed around 100 K for the sample with 5 nm NiO. The peak could be associated with the spin transport properties of bulk and interfaces in the heterostructure at different temperatures, as discussed in the previous section. Further, field-dependent experiments revealed that the SSE response follows a Brillouin function with a spin S=7/2 at low temperatures. The experimental results indicate that the GGG substrate could generate a large flow of spin currents due to paramagnetic SSE when a strong magnetic field is applied at low temperatures.[31]

V. SUMMARY

In summary, the spin transport properties of an insulating tri- layer based on two ferrimagnetic insulators separated by a thin anti- ferromagnetic insulator were presented. The spin diffusion length of NiO was found to be $\lambda_{NiO} \simeq 3.8$ nm at room temperature. The ther- mally injected spin current generated from the bottom YIG layer is larger than expected, which suggests an enhancement of spin current by the NiO layer or its interfaces. In addition, the SSE voltages show a broad peak around 100 K. The underlying physics of this peak was discussed, addressing the competing effects of magnon popula- tion and effective magnon propagation length in a ferrimagnet, spin conductance at the FI/AFI and AFI/NM interfaces, and the enhance- ment of spin currents near the blocking temperature of an antiferro- magnet. In addition, a large increase of the SSE signal was observed at low temperatures, indicating the non-trivial effects from the GGG substrate. Following field-dependent experiments suggest that the increase of the SSE signal may be associated with the paramagnetic SSE of the GGG substrate when a strong magnetic field was applied. This experimental study provides information on how spins can be generated, transported and detected in a heterostructure consisting of paramagnetic, ferrimagnetic and antiferromagnetic insulators.

SUPPLEMENTARY MATERIAL

The supplementary material provides the details of sample characterization by scanning electron microscopy (STEM), Vibrat- ing Sample Magnetometer (VSM), transport measurements of a GGG/YIG/Pt sample, and field-dependent measurements of a GGG/YIG/NiO/YIG/Pt sample above 50 K.

ACKNOWLEDGMENTS

This work was supported partially by the MRSEC Program of the National Science Foundation under Award Number DMR- 1420073. The instrumentation used in this research was support in part by the Gordon and Betty Moore Foundation EPiQS Ini- tiative through Grant GBMF4838 and in part by the National Sci- ence Foundation under award NSF-DMR-1531664. ADK received support from the National Science Foundation under Grant No. DMR-1610416. JD and MW were supported by the U. S. National Science Foundation under Grants No. EFMA-1641989 and No. ECCS-1915849. Sandia National Laboratories is a multi-program laboratory

managed and operated by National Technology and Engineering Solutions of Sandia, LLC., a wholly owned subsidiary of Honeywell International, Inc., for the U.S. Department of Energy's National Nuclear Security Administration under contract DE-NA- 0003525. The views and conclusions contained herein are those of the authors and should not be interpreted as necessarily representing the official policies or endorsements, either expressed or implied, of the U.S. Government. We also would like to express our thanks to Pradeep Manandhar from Spin Memory Inc. for TEM characterization. We also want to thank Mingxin He from CSMR in New York University for his help.

REFERENCES

[1]M. N. Baibich, J. M. Broto, A. Fert, F. Nguyen Van Dau, F. Petroff, P. Etienne, G. Creuzet, A. Friederich, and J. Chazelas, "Giant magnetoresistance of (001) Fe/(001) Cr magnetic superlattices," Phys. Rev. Lett. **61**, 2472 (1988).

[2] G. Binasch, P. Grünberg, F. Saurenbach, and W. Zinn, "Enhanced magnetoresis- tance in layered magnetic structures with antiferromagnetic interlayer exchange," Phys. Rev. B **39**, 4828 (1989).

[3]L. Berger, "Emission of spin waves by a magnetic multilayer traversed by a current," Phys. Rev. B **54**(13), 9353 (1996).

[4]J. C. Slonczewski, "Excitation of spin waves by an electric current," Journal of Magnetism and Magnetic Materials **195**(2), L261–L268 (1999).

[5] T. Kimura, Y. Otani, T. Sato, S. Takahashi, and S. Maekawa, "Room-temperature reversible spin Hall effect," Phys. Rev. Lett. **98**, 156601 (2007).

[6]M. I. Dyakonov and V. I. Perel, "Current-induced spin orientation of electrons in semiconductors," Phys. Lett. A **35**(6), 459–460 (1971).

[7]J. E. Hirsch, "Spin Hall effect," Phys. Rev. Lett. **83**(9), 1834 (1999).

[8]S. Zhang, "Spin Hall effect in the presence of spin diffusion," Phys. Rev. Lett. **85**(2), 393 (2000).

[9]C. F. Pai, L. Liu, Y. Li, H. W. Tseng, D. C. Ralph, and R. A. Buhrman, "Spin transfer torque devices utilizing the giant spin Hall effect of tungsten," Appl. Phys. Lett. **101**, 122404 (2012).

[10] Y. Tserkovnyak, A. Brataas, and G. E. Bauer, "Enhanced Gilbert damping in thin ferromagnetic films," Phys. Rev. Lett. **88**(11), 117601 (2002).

[11]K. Uchida, S. Takahashi, K. Harii, J. Ieda, W. Koshibae, K. Ando, S. Maekawa, and E. Saitoh, "Thermal spin pumping and magnon-phonon-mediated spin- Seebeck effect," Nature **455**, 778 (2008).

[12] K. Uchida, H. Adachi, T. Ota, H. Nakayama, S. Maekawa, and E. Saitoh, "Obser- vation of longitudinal spin-Seebeck effect in magnetic insulators," Appl. Phys. Lett. **97**(17), 172505 (2010).

[13]C. M. Jaworski, J. Yang, S. Mack, D. D. Awschalom, J. P. Heremans, and R. C. Myers, "Observation of the spin-Seebeck effect in a ferromagnetic semiconduc- tor," Nature Materials **9**(11), 898 (2010).

[14]S. M. Wu, W. Zhang, K. C. Amit, P. Borisov, J. E. Pearson, J. S. Jiang, D. Leder- man, A. Hoffmann, and A. Bhattacharya, "Antiferromagnetic spin Seebeck effect," Phys. Rev. Lett. **116**(9), 097204 (2016).

[15]B. Dieny, V. S. Speriosu, S. Metin, S. S. Parkin, B. A. Gurney, P. Baumgart, and D. R. Wilhoit, "Magnetotransport properties of magnetically soft spin-valve structures," Journal of Applied Physics **69**(8), 4774–4779 (1991).

[16]F. J. Jedema, A. T. Filip, and B. J. Van Wees, "Electrical spin injection and accu- mulation at room temperature in an all-metal mesoscopic spin valve," Nature **410**(6826), 345 (2001).

[17]Y. Cheng, K. Chen, and S. Zhang, "Giant magneto-spin-Seebeck effect and magnon transfer torques in insulating spin valves," Appl. Phys. Lett. **112**, 052405 (2018).

[18]R. Cheng, D. Xiao, and J. G. Zhu, "Antiferromagnet-based magnonic spin- transfer torque," Phys. Rev. B **98**, 020408(R) (2018).

[19]C. Y. Guo, C. H. Wan, X. Wang, C. Fang, P. Tang, W. J. Kong, M. K. Zhao, L. N. Jiang, B. S. Tao, G. Q. Yu, and X. F. Han, "Magnon valves based on YIG/NiO/YIG all-insulating magnon junctions," Phys. Rev. B **98**(13), 134426 (2018).

[20]B. Heinrich, C. Burrowes, E. Montoya, B. Kardasz, E. Girt, Y. Song, Y. Sun, and M. Wu, "Spin pumping at the magnetic insulator (YIG)/normal metal (Au) interfaces," Phys. Rev. Lett. **107**, 066604 (2011).

[21]D. Wesenberg, T. Liu, D. Balzar, M. Wu, and B. L. Zink, "Long-distance spin transport in a disordered magnetic insulator," Nature Physics **13**, 987 (2017). [22]P. W. Palmberg, R. E. DeWames, and L. A. Vredevoe, "Direct observation of coherent exchange scattering by low-energy electron diffraction from antiferro- magnetic NiO," Phys. Rev. Lett. **21**, 682 (1968).

[23] W. Lin, K. Chen, S. Zhang, and C. L. Chien, "Enhancement of thermally injected spin current through an antiferromagnetic insulator," Phys. Rev. Lett. **116**, 186601 (2016).

[24]J. Holanda, D. S. Maior, O. Alves Santos, L. H. Vilela-Leão, J. B. S. Mendes, A. Azevedo, R. L. Rodríguez-Suárez, and S. M. Rezende, "Spin Seebeck effect in the antiferromagnet nickel oxide at room temperature," Appl. Phys. Lett. **111**(17), 172405 (2017).

[25]S. M. Rezende, R. L. Rodrguez-Surez, R. O. Cunha, A. R. Rodrigues, F. L. A. Machado, G. A. Fonseca Guerra, J. C. Lopez Ortiz, and A. Azevedo, "Magnon spin-current theory for the longitudinal spin-Seebeck effect," Phys. Rev. B **89**(1), 014416 (2014).

[26] S. M. Rezende, R. L. Rodrguez-Surez, and A. Azevedo, "Diffusive magnonic spin transport in antiferromagnetic insulators," Phys. Rev. B **93**, 054412 (2016).

[27]H. Wang, C. Du, P. C. Hammel, and F. Yang, "Antiferromagnonic spin trans- port from $Y_3Fe_5O_{12}$ into NiO," Phys. Rev. Lett. **113**, 097202 (2014).

[28]W. Lin and C. L. Chien, "Electrical detection of spin backflow from an antifer- romagnetic insulator/$Y_3Fe_5O_{12}$ interface," Phys. Rev. Lett. **118**, 067202 (2017). [29]P. Schiffer, A. P. Ramirez, D. A. Huse, P. L. Gammel, U. Yaron, D. J. Bishop, and A. J. Valentino, "Frustration

induced spin freezing in a site-ordered magnet: Gadolinium gallium garnet," Phys. Rev. Lett. **74**(12), 2379 (1995).

[30] K. Oyanagi, S. Takahashi, L. J. Cornelissen, J. Shan, S. Daimon, T. Kikkawa, G. E. W. Bauer, B. J. van Wees, and E. Saitoh, "Efficient spin transport in a paramagnetic insulator," arXiv:1811.11972 (Nov. 2018).
[31] S. M. Wu, J. E. Pearson, and A. Bhattacharya, "Paramagnetic spin Seebeck effect," Phys. Rev. Lett. **114**(18), 186602 (2015).

[32] H. Chang, P. Li, W. Zhang, T. Liu, A. Hoffmann, L. Deng, and M. Wu, "Nanometer-thick yttrium iron garnet films with extremely low damping," IEEE Magn. Lett. **5**, 6700104 (2014).
[33] Y. Chen, D. Roy, E. Cogulu, H. Chang, M. Wu, and A. D. Kent, "First harmonic measurements of the spin Seebeck effect," Appl. Phys. Lett. **113**, 202403 (2018). [34] Y. Chen, "Spin transport in magnetic insulators," Ph.D. thesis, New York University, ProQuest Dissertations Publishing, 13420488 (2019).

[35] Y. Hung, C. Hahn, H. Chang, M. Wu, H. Ohldag, and A. D. Kent, "Spin transport in antiferromagnetic NiO and magnetoresistance in $Y_3Fe_5O_{12}$ /NiO/Pt structures," AIP Advances **7**(5), 055903 (2017).
[36] S. S.-L. Zhang and S. Zhang, "Magnon mediated electric current drag across a ferromagnetic insulator layer," Phys. Rev. Lett. **109**, 096603 (2012).

[37] E. J. Guo, J. Cramer, A. Kehlberger, C. A. Ferguson, D. A. MacLaren, G. Jakob, and M. Kläui, "Influence of thickness and interface on the low-temperature enhancement of the spin Seebeck effect in YIG films," Phys. Rev. X **6**(3), 031012 (2016).

Figure Captions

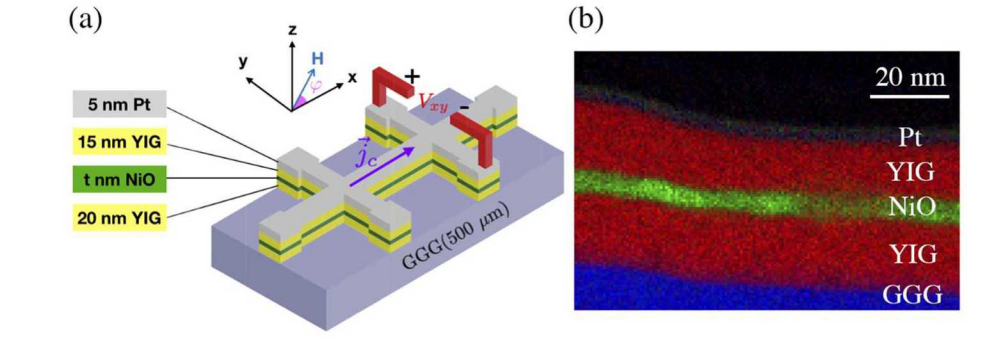

FIG. 1. A schematic of the sample and cross-sectional characterization of the sample by scanning transmission electron microscope energy-dispersive X-ray spectroscopy (STEM-EDS). (a) Sample geometry showing the layers, the electrical contacts and the applied magnetic field. $\vec{j}c$ is the density of the charge current applied in the x-direction. V_{xy} is the voltage measured in the transverse direction, and φ is the angle between the applied magnetic field and the current. GGG,

YIG, NiO, and Pt are represented as light purple, yellow, green, and grey, respectively. (b) Sample cross section characterized by STEM-EDS. GGG, YIG, NiO, and Pt layers are colored in blue, red, green, and dark gray, respectively.

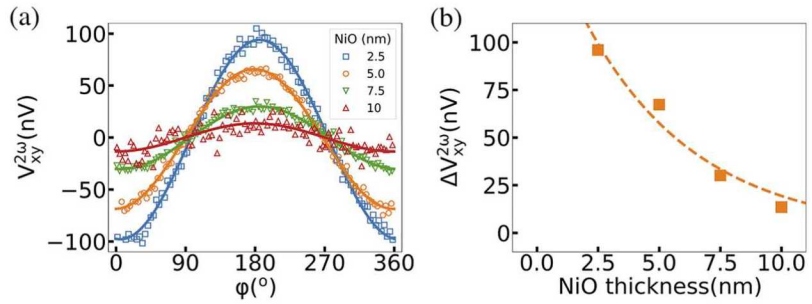

FIG. 2. Angular dependence and NiO thickness depen- dence of $V^{2\omega}$ *xy* measured with an in-plane magnetic field of 0.4 T at room temperature. (a) Angular dependence of $V^{2\omega}$ with an AC density of $j_{ac} = 1.5 \times 10^{10}$ A/m^2. Δ $V^{2\omega}$ *xy* is extracted by fitting the curve with a cosine function. (b) Δ $V^{2\omega}$ *xy* as a function of the NiO thickness. The curve is fitted with $V = V_{bottom} e^{-t/\lambda_{NiO}} + V_{top}$, where $V_{bottom} = 172 \pm 39$ nV and the spin diffusion length of NiO is $\lambda_{NiO} \approx 3.8 \pm 0.9$ nm with $V_{top} \equiv 10$ nV.

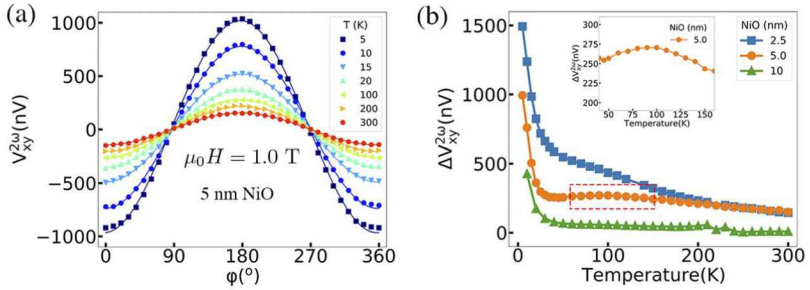

FIG. 3. Second harmonic response $V^{2\omega}$ *xy* measured at several temperatures with an applied magnetic field μ0 *H* = 1.0 T for NiO thicknesses of 2.5, 5, and 10 nm. (a) Angular dependence of $V^{2\omega}$ *xy* measured from 5 to 300 K. Note that the angle φ is defined in Fig. 1(a). (b) Δ $V^{2\omega}$ *xy* measured as a function of the temperature. Inset: a broad peak is observed around 100 K for the sample with a 5 nm NiO thickness.

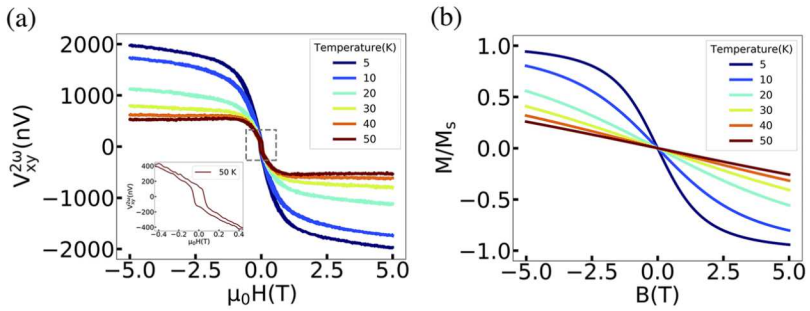

FIG. 4. (a) Field dependence of the $V^{2\omega}$ *xy* measured between 5 and 50 K, with φ = 0 . The sample is GGG (500 μm)/YIG(20 nm)/NiO(2.5 nm)/YIG(15 nm)/Pt (5 nm). The magnetic field is swept between -5 and +5 T. The offset of $V^{2\omega}$ *xy* has been removed. (b) Brillouin function of an S=7/2 spin.